CENTER FOR ADVANCED RESEARCH IN FINANCE

CARF Working Paper

CARF-F-536

Moments of Maximum of Lévy Processes: Application to Barrier and Lookback Option Pricing

Yuan Li
Graduate School of Economics, University of Tokyo

Kenichiro Shiraya
Graduate School of Economics, University of Tokyo

Yuji Umezawa

Akira Yamazaki
Graduate School of Business Administration, Hosei University

March 30, 2022

CARF is presently supported by Nomura Holdings, Inc., Sumitomo Mitsui Banking Corporation, The Dai-ichi Life Insurance Company, Limited, The Norinchukin Bank, MUFG Bank, Ltd. and Ernst & Young ShinNihon LLC. This financial support enables us to issue CARF Working Papers.

Moments of Maximum of Lévy Processes:
Application to Barrier and Lookback Option Pricing

Yuan Li* Kenichiro Shiraya† Yuji Umezawa Akira Yamazaki‡

March 30, 2022

Abstract

We propose an analytical method to calculate mixed moments between the terminal value and the maximum of a Lévy process. The method derives the moments directly from the Wiener-Hopf factors without finding density or characteristic functions. The advantage of this method is that it is computationally fast and stable. Furthermore, it can be applied to a wide class of Lévy processes. Numerical experiments show that our method provides sufficiently accurate values of the moments. We then apply it to a Monte Carlo simulation for the pricing of barrier and lookback options. The results show that our simulation method can greatly reduce the time discretization error.

Keywords: Lévy processes, moments of maximum, Wiener-Hopf factorization, Monte Carlo simulation, discretization error, barrier option, lookback option

*Graduate School of Economics, University of Tokyo.

†Graduate School of Economics, University of Tokyo. Kenichiro Shiraya is supported by CARF (Center for Advanced Research in Finance) at University of Tokyo.

‡Graduate School of Business Administration, Hosei University. Akira Yamazaki gratefully acknowledges the financial support from JSPS KAKENHI, Grant Number 21K01585. His work is also supported by the Research Institute for Innovation Management at Hosei University.

1 Introduction

The Lévy processes are a class of continuous-time stochastic processes with discontinuous trajectories. They are not only capable of representing various types of jumps in paths but also have properties that make them tractable for analysis. Their application fields are vast, including physics, stochastic control problems, queueing theory, insurance, and finance.

However, the maximum of a Lévy process is notorious for being difficult to analyze. Even though there is a well-known analytical representation for the maximum called *the Wiener-Hopf factorization*, it is not easy to use it in practice. There are only a few Lévy processes, such as Brownian motion, for which the Wiener-Hopf factors can be obtained in closed form. Unfortunately, it is very difficult to calculate the probability distribution of the maximum from the Wiener-Hopf factorization numerically. For numerical calculation, in addition to the need to obtain the Wiener-Hopf factors numerically, the inverse Laplace transform and the double inverse Fourier transform are necessary. This procedure is computationally slow, and the results are unstable. In fact, only a group of Lévy processes, known as *the spectrally negative Lévy processes*, can be implemented in such numerical calculation. A spectrally negative Lévy process has only negative jumps with a diffusion term. Madan and Schoutens (2007), Jönsson and Schoutens (2008), and Ozeki et al. (2011) applied the spectrally negative Lévy processes to finance, but the scope of their applications is limited due to the specificity of the processes.

Another approach to the maximum of a Lévy process is Monte Carlo simulations. In a Monte Carlo simulation, a number of paths of the Lévy process are generated, and the maximum value in each path is collected as a sample. For example, if we want to find the expected value of the maximum, we can take the average of the samples of the maximum. However, there are two problems with this approach. The first is the convergence error, which is caused by the difference between the population mean and the sample mean of the Monte Carlo simulation. In order to reduce this error, a large number of samples have to be generated. The second is the discretization error. When simulating a Lévy process, its sample paths have to be discretized in time. This discretization causes a bias because the sample of the maximum is always smaller than the true maximum. In order to eliminate this error, a finer discretization is necessary. In general, Monte Carlo simulations are time-consuming, and there is a tradeoff between reducing these two errors and computation time.

We develop an analytical method to calculate the moments of the maximum of a Lévy process. In our method, the moments of the maximum are derived directly from the Wiener-Hopf factors, to circumvent finding its density function or characteristic function. A series of mixed moments between the terminal value and the maximum of a Lévy process can be obtained recursively. The advantage of our method is that the double inverse Fourier transform is no longer necessary in numerical calculations. As a result, the numerical results can be obtained faster and more stable. Our method is applicable to a class of Lévy processes that are widely used in applications.

Moments are only fragmentary information of a probability distribution, but their applications are quite broad. We propose an application of the moments of the maximum to the pricing of barrier and lookback options in finance.

The pricing of path-dependent options under Lévy processes has been studied vigorously in past literature. However, only a few analytical methods have been discovered. For example, Feng and Linetsky (2008) applied the Hilbert transform to price discretely monitored barrier options. Fusai and Meucci (2008) derived semi-analytical formulas for geometric average option prices. Yamazaki (2014) applied the Gram-Charlier expansion to price arithmetic average options. Umezawa and Yamazaki (2015) provided a semi-analytical formula, which is based on multivariate characteristic functions, for some path-dependent option

prices with discrete monitoring. Unfortunately, as far as the existing research is concerned, it may be difficult to find an analytical method for pricing barrier and lookback options *with continuous monitoring*.

In practice, Monte Carlo simulations are used to price barrier and lookback options that are continuously monitored. We propose an efficient Monte Carlo simulation combined with our method of moment calculation. Our simulation method can considerably reduce the discretization error in option price estimates. This improvement allows for a significant reduction in computation time.

There are a number of techniques for improving Monte Carlo option pricing under Lévy processes. For example, Avramidis et al. (2003), Avramidis et al. (2006), Becker (2010), Shiraya et al. (2020), and Shiraya et al. (2021) proposed variance reduction, which is a technique for reducing the convergence error. Avramidis et al. (2003), Ribeiro and Webber (2004), Avramidis et al. (2006), and Becker (2010) developed a bridge sampling technique to eliminate the discretization error, but its application is limited to a specific Lévy process. Our error reduction method, on the other hand, has a much wider range of applications.

The rest of the paper is organized as follows. Section 2 provides the definition of the Lévy process and its maximum. Section 3 presents an analytical method for calculating the moments of the maximum. In Section 4, numerical experiments are conducted to confirm the validity of our method. Section 5 proposes an application of our method to evaluate barrier and lookback options. Section 6 refers to the conclusion. In Appendix, we provide some technical supplements.

2 Lévy Process and Its Maximum

We start with a probability space $(\Omega, \mathcal{F}, \mathbb{Q})$ carrying a one-dimensional Lévy process $(Y_t)_{t\geq 0}$ with the associated filtration $\mathbb{F} := (\mathcal{F}_t)_{t\geq 0}$. A stochastic process $(Y_t)_{t\geq 0}$ on $(\Omega, \mathcal{F}, \mathbb{Q})$ with values in $\mathbf{R}$ such that $Y_0 = 0$ is called a Lévy process if it possesses the following properties: (1) $(Y_t)_{t\geq 0}$ is $\mathbb{F}$-adapted. (2) The sample paths of $(Y_t)_{t\geq 0}$ are right continuous with left limits. (3) $Y_u - Y_t$ is independent of $\mathcal{F}_t$ for $0 \leq t < u$. (4) $Y_u - Y_t$ has the same distribution as Y_{u-t} for $0 \leq t < u$.

The following proposition, which is named *the Lévy-Khintchine formula*, gives the general representation of the characteristic function of an arbitrary Lévy process. The proof of the proposition can be found on pp.35-45 in Sato (1999) for instance.

Proposition 1 *(Lévy-Khintchine formula) Let $(Y_t)_{t\geq 0}$ be a Lévy process on $\mathbf{R}$. The characteristic function of the distribution of Y_t has the form*

$$\phi_{Y_t}(\theta) := \mathbb{E}\left[e^{i\theta Y_t}\right] = e^{-t\psi_Y(\theta)}, \quad t \geq 0, \ \ \theta \in \mathbf{R}, \tag{2.1}$$

where the function ψ_Y, which is called the characteristic exponent, is given by

$$\psi_Y(\theta) = -ia\theta + \frac{1}{2}b^2\theta^2 + \int_{-\infty}^{\infty}(1 - e^{i\theta y} + i\theta y \mathbf{1}_{|y|<1})\Pi(dy). \tag{2.2}$$

Here $a \in \mathbf{R}$ and $b \geq 0$ are constants, and Π is a positive Radon measure on $\mathbf{R}\setminus\{0\}$ verifying

$$\int_{-\infty}^{\infty}(1 \wedge y^2)\Pi(dy) < \infty.$$

The parameter b^2 is called *the Gaussian coefficient*, and the measure Π is called *the Lévy measure*. The triplet (a, b^2, Π) is referred to as *the Lévy characteristics*. Intuitively, a and b^2

represent the drift and the variance of the continuous component of the process, respectively. The Lévy measure determines the property of the jump component of the process. If $\Pi = 0$, the Lévy process is identified as a Gaussian process. If $a = b = 0$, the Lévy process becomes a pure jump process with no continuous component.

There is a class of Lévy processes called *the finite-activity jump processes*, which make a finite number of jumps within any finite time interval. An arbitrary finite-activity jump process can be represented as a compound Poisson process. In option pricing, Merton (1976) employed the compound Poisson process with normally distributed jumps, and Kou (2002) adopted that with double-exponentially distributed jumps. Eraker et al. (2003) and Eraker (2004) applied the compound Poisson process with one-side exponentially distributed jumps to the empirical analysis of option markets.

Another important class of Lévy processes is *the infinite-activity jump processes*, which generate an infinite number of jumps within any finite time interval. Examples of this class include the normal inverse Gaussian process by Barndorff-Nielsen (1997), the variance gamma process by Madan and Seneta (1990) and Madan et al. (1998), the finite moment log-stable process by Carr and Wu (2003), the Meixner process by Schoutens (2002), and the CGMY process by Carr et al. (2002).

For more details on the Lévy processes as applied to finance, see Cont and Tankov (2003) and Boyarchenko and Levendorskiĭ (2002).

The maximum and the minimum of a Lévy process in time interval $[0, T]$ are written as

$$\overline{Y}_T := \sup_{0 \le t \le T} Y_t \qquad \text{and} \qquad \underline{Y}_T := \inf_{0 \le t \le T} Y_t,$$

respectively. In the following, we only discuss the maximum, but the minimum can be analyzed in a similar way to the maximum.

3 Mixed Moments

In this section, we provide a formula for calculating mixed moments between the terminal value and the maximum of a Lévy process. Let the (n_1, n_2)-th mixed moment of $(Y_T, \overline{Y}_T)$ denote

$$m_{n_1,n_2} := \mathbb{E}\left[(Y_T)^{n_1} \left(\overline{Y}_T\right)^{n_2} \right],$$

for $n_1, n_2 \in \{0, 1, 2, \dots\}$.

3.1 Brownian Motion and Its Maximum

Let $Z_t := at + bW_t$, where $(W_t)_{t \ge 0}$ is a one-dimensional standard Brownian motion, and a and $b > 0$ are some constants. Note that the drifted Brownian motion $(Z_t)_{t \ge 0}$ is a special case of Lévy processes. The joint characteristic function of $(Z_T, \overline{Z}_T)$ is known to be given in the form

$$\begin{aligned}
\phi_{Z_T,\overline{Z}_T}(\theta_1, \theta_2) &:= \mathbb{E}\left[e^{i\theta_1 Z_T + i\theta_2 \overline{Z}_T} \right] \\
&= \frac{1}{2} e^{\frac{\zeta^2 - a^2}{2b^2} T} \left\{ 1 + \frac{ib^2\theta_2}{2\zeta - ib^2\theta_2} \right\} \left\{ 1 + \operatorname{erf}\left(\sqrt{\frac{T}{2b^2}} \zeta \right) \right\} \\
&\quad + \frac{1}{2} e^{\frac{\eta^2 - a^2}{2b^2} T} \left\{ 1 - \frac{ib^2\theta_2}{2\eta + ib^2\theta_2} \right\} \left\{ 1 - \operatorname{erf}\left(\sqrt{\frac{T}{2b^2}} \eta \right) \right\}, \quad \theta_1, \theta_2 \in \mathbf{R},
\end{aligned}$$

where $\zeta := \zeta(\theta_1, \theta_2) = a + ib^2(\theta_1 + \theta_2)$, $\eta := \eta(\theta_1) = a + ib^2\theta_1$, and

$$\mathrm{erf}(x) := \frac{2}{\sqrt{\pi}} \int_0^x e^{-u^2} du,$$

which is the error function. Therefore, the (n_1, n_2)-th mixed moment of $(Z_T, \overline{Z}_T)$ denoted by $\hat{m}_{n_1,n_2}$ is obtained by[1]

$$\hat{m}_{n_1,n_2} = i^{-(n_1+n_2)} (\partial_{n_1,n_2} \phi_{Z_T,\overline{Z}_T})(0,0).$$

3.2 Lévy Process and Its Maximum

In this subsection, it is shown that the Wiener-Hopf factorization can be used to find mixed moments of $(Y_T, \overline{Y}_T)$ of a Lévy process $(Y_t)_{t\geq 0}$. First, we introduce the Wiener-Hopf factors in the following lemma. The proof of the lemma can be found on p.334 of Sato (1999).

Lemma 1 *Let $q > 0$. There exist a unique pair of characteristic functions of infinitely divisible distributions supported on $[0, \infty)$ and $(-\infty, 0]$, which are denoted by Φ_q^+ and Φ_q^-, respectively, such that*

$$\frac{q}{q + \psi_Y(\theta)} = \Phi_q^+(\theta)\Phi_q^-(\theta), \quad \theta \in \mathbf{R}.$$

These functions are represented as

$$\Phi_q^+(\theta) = \exp\left\{ \int_0^{+\infty} T^{-1} e^{-qT} dT \int_0^{+\infty} \left(e^{i\theta x} - 1\right) dF_{Y_T}(x) \right\}, \tag{3.1}$$

$$\Phi_q^-(\theta) = \exp\left\{ \int_0^{+\infty} T^{-1} e^{-qT} dT \int_{-\infty}^{0} \left(e^{i\theta x} - 1\right) dF_{Y_T}(x) \right\}, \tag{3.2}$$

where $F_{Y_T}(\cdot)$ is the cumulative distribution function of Y_T.

The functions Φ_q^+ and Φ_q^- are known as the *Wiener-Hopf factors*. Φ_q^+ can be continuously extended to a bounded analytic function without zeros on the upper half plane. Φ_q^- can also be extended to the lower half plane.

The following lemma shows that the Laplace transform of the joint characteristic function of $(Y_T, \overline{Y}_T)$ can be represented as the product of the Wiener-Hopf factors. The proof of the lemma can be found on p.341 of Sato (1999).

Lemma 2 *Let*

$$\phi_{Y_T,\overline{Y}_T}(\theta_1, \theta_2) := \mathbb{E}\left[e^{i\theta_1 Y_T + i\theta_2 \overline{Y}_T} \right], \quad \theta_1, \theta_2 \in \mathbf{R}, \tag{3.3}$$

be the joint characteristic function of $(Y_T, \overline{Y}_T)$. The Laplace transform in T of $\phi_{Y_T,\overline{Y}_T}$ is given by

$$q \int_0^{+\infty} e^{-qT} \phi_{Y_T,\overline{Y}_T}(\theta_1, \theta_2) dT = \Phi_q^+(\theta_1 + \theta_2)\Phi_q^-(\theta_1),$$

for any $q > 0$.

[1] The partial derivative of a function f in x and y is denoted by

$$(\partial_{n_1,n_2} f)(x, y) := \frac{\partial^{n_1+n_2} f}{\partial x^{n_1} \partial y^{n_2}}(x, y), \quad n_1, n_2 \in \{0, 1, 2, \dots\}.$$

Closed-form expressions for the Wiener-Hopf factors are not known, except in a few special cases. To obtain the Wiener-Hopf factors, some numerical calculation is required. However, the calculations of (3.1) and (3.2) are inefficient because they involve the cumulative distribution function of Y_T, which is usually unknown in closed form. Therefore, it is difficult, even numerically, to obtain the joint characteristic function (3.3) by Lemma 2. This problem has been recognized as a bottleneck in analyzing the maximum of Lévy processes.

Our idea is to calculate directly mixed moments between the terminal value and the maximum of a Lévy process without having to find the joint characteristic function. The following proposition gives us the representation of the Laplace transform to the mixed moments of $(Y_T, \overline{Y}_T)$.

Proposition 2 *Let $D^{(n)}\Phi_q^{\pm}$ be the n-th derivative of $\Phi_q^{\pm}(\theta)$ with respect to parameter θ. The Laplace transform in T of the mixed moment m_{n_1,n_2} is given by*

$$q\int_0^{+\infty} e^{-qT} m_{n_1,n_2} dT = i^{-(n_1+n_2)} \sum_{k=0}^{n_1} \binom{n_1}{k} \left(D^{(n_2+k)}\Phi_q^{+}\right)(0) \left(D^{(n_1-k)}\Phi_q^{-}\right)(0), \quad (3.4)$$

for any $q > 0$.

Proof of Proposition 2: From Lemma 2, we have

$$\begin{aligned} q\int_0^{+\infty} e^{-qT} \left(\partial_{n_1,n_2}\phi_{Y_T,\overline{Y}_T}\right)(0,0) dT &= \partial_{n_1,n_2}\left(\Phi_q^{+}(\theta_1+\theta_2)\Phi_q^{-}(\theta_1)\right)\Big|_{\theta_1,\theta_2=0} \\ &= \frac{\partial^{n_1}}{\partial\theta_1^{n_1}}\left(D^{(n_2)}\Phi_q^{+}\right)(\theta_1+\theta_2)\,\Phi_q^{-}(\theta_1)\Big|_{\theta_1,\theta_2=0} \\ &= \sum_{k=0}^{n_1}\binom{n_1}{k}\left(D^{(n_2+k)}\Phi_q^{+}\right)(0)\left(D^{(n_1-k)}\Phi_q^{-}\right)(0). \end{aligned}$$

□

Boyarchenko and Levendorskiĭ (2002) provided an expression for the Wiener-Hopf factor that can be calculated more efficiently. It is valid for the tempered stable process, the normal inverse Gaussian process, and other suitable processes. According to them, the Wiener-Hopf factors can be represented as

$$\Phi_q^{+}(\theta) = e^{\theta\varphi_q^{+}(\theta)} \quad \text{and} \quad \Phi_q^{-}(\theta) = e^{\theta\varphi_q^{-}(\theta)}, \quad (3.5)$$

where

$$\varphi_q^{+}(\theta) := \frac{1}{2\pi i}\int_{-\infty+i\omega_-}^{+\infty+i\omega_-} \frac{\ln(q+\psi_Y(z))}{z(\theta-z)}dz, \quad \varphi_q^{-}(\theta) := -\frac{1}{2\pi i}\int_{-\infty+i\omega_+}^{+\infty+i\omega_+} \frac{\ln(q+\psi_Y(z))}{z(\theta-z)}dz,$$

with some $\omega_- < 0$ and $\omega_+ > 0$ such that Φ_q^{+} and Φ_q^{-} are analytic in the half plane $\Im\theta > \omega_-$ and $\Im\theta < \omega_+$, respectively.

By assuming the Boyarchenko-Levendorskiĭ representation (3.5), we can obtain the following proposition to calculate $D^{(n)}\Phi_q^{\pm}$ in Proposition 2.

Proposition 3 *Suppose that the Wiener-Hopf factors of a Lévy process $(Y_t)_{t\geq 0}$ have the Boyarchenko-Levendorskiĭ representation (3.5). Then we have*

$$\left(D^{(n+1)}\Phi_q^{\pm}\right)(0) = \sum_{k=0}^{n}(1+k)\binom{n}{k}\left(D^{(k)}\varphi_q^{\pm}\right)(0)\left(D^{(n-k)}\Phi_q^{\pm}\right)(0), \quad (3.6)$$

where $\left(D^{(n)}\varphi_q^{\pm}\right)(\theta)$ *denotes the* n*-th derivative of* $\varphi_q^{\pm}$ *in parameter* θ*. The* n*-th derivative at* $\theta = 0$ *is given by*

$$\left(D^{(n)}\varphi_q^{+}\right)(0) = (-1)^n \frac{n!}{2\pi i}\int_{-\infty+i\omega_-}^{+\infty+i\omega_-} \frac{\ln(q+\psi_Y(z))}{z^{n+2}}dz, \tag{3.7}$$

$$\left(D^{(n)}\varphi_q^{-}\right)(0) = (-1)^{n+1} \frac{n!}{2\pi i}\int_{-\infty+i\omega_+}^{+\infty+i\omega_+} \frac{\ln(q+\psi_Y(z))}{z^{n+2}}dz, \tag{3.8}$$

with $\left(D^{(0)}\Phi_q^{\pm}\right)(0) := \Phi_q^{\pm}(0) = 1$.

Proof of Proposition 3: Consider a sequence of functions $(g_n)_{n\geq 0}$ such that

$$\left(D^{(n)}\Phi_q^{+}\right)(\theta) = g_n(\theta)\Phi_q^{+}(\theta), \quad \text{for } n = 0, 1, 2, \ldots. \tag{3.9}$$

Obviously, $g_0(\theta) = 1$ and $g_1(\theta) = \varphi_q^{+}(\theta) + \theta\left(D\varphi_q^{+}\right)(\theta)$ for any $\theta \in \mathbf{R}$. The n-th derivative of g_1 is given by

$$\begin{aligned} g_1^{(n)}(\theta) &= \left(D^{(n)}\varphi_q^{+}\right)(\theta) + \frac{d^n}{d\theta^n}\theta\left(D\varphi_q^{+}\right)(\theta) \\ &= \left(D^{(n)}\varphi_q^{+}\right)(\theta) + \sum_{k=0}^{n}\binom{n}{k}\theta^{(k)}\left(D^{(n-k+1)}\varphi_q^{+}\right)(\theta) \\ &= (n+1)\left(D^{(n)}\varphi_q^{+}\right)(\theta) + \theta\left(D^{(n+1)}\varphi_q^{+}\right)(\theta). \end{aligned}$$

By the definition of g_n in (3.9), we have

$$\begin{aligned} \left(D^{(n+1)}\Phi_q^{+}\right)(\theta) &= \frac{d^n}{d\theta^n}g_1(\theta)\Phi_q^{+}(\theta) = \sum_{k=0}^{n}\binom{n}{k}g_1^{(k)}(\theta)\left(D^{(n-k)}\Phi_q^{+}\right)(\theta) \\ &= \left(\sum_{k=0}^{n}\binom{n}{k}g_1^{(k)}(\theta)g_{n-k}(\theta)\right)\Phi_q^{+}(\theta). \end{aligned} \tag{3.10}$$

Note that

$$g_{n+1}(0) = \sum_{k=0}^{n}\binom{n}{r}g_1^{(k)}(0)g_{n-k}(0) = \sum_{k=0}^{n}(1+k)\binom{n}{k}\left(D^{(k)}\varphi_q^{+}\right)(0)g_{n-k}(0). \tag{3.11}$$

Substituting (3.11) and $\Phi_q^{+}(0) = 1$ into (3.10), and noting $\left(D^{(n)}\Phi_q^{+}\right)(0) = g_n(0)$, we obtain (3.6) for $\left(D^{(n)}\Phi_q^{+}\right)(0)$. Similarly, we can also show (3.6) for $\left(D^{(n)}\Phi_q^{-}\right)(0)$. □

4 Numerical Experiments

In this section, we demonstrate the validity of our moment calculation method proposed in the previous section. Let us consider a Lévy process $(Y_t)_{t\geq 0}$ given by

$$Y_t = (r + \psi_X(-i))t + X_t, \quad \text{for any } t \geq 0, \tag{4.1}$$

where r is a constant, and $(X_t)_{t\geq 0}$ is the normal inverse Gaussian (NIG) process. The characteristic exponent of the NIG process is

$$\psi_X(\theta) = \frac{1}{\kappa}\sqrt{1 + \sigma^2\kappa\theta^2 - 2i\mu\kappa\theta} - \frac{1}{\kappa}, \tag{4.2}$$

Table 1: Model parameters

	r	σ	μ	κ
Case 1	0.03	0.20	-0.18	0.06
Case 2	0.03	0.20	-0.18	0.20

where σ, μ, κ are some constants. The NIG process is a time-changed Brownian motion subordinated by the inverse Gaussian process. This process has an infinite variation with high frequency of small jumps and is one of the most commonly used Lévy processes in finance applications. Parameter σ determines the standard deviation of the distribution of X_1, parameter μ controls the skewness, and parameter κ generates the excess kurtosis. The NIG process converges to a Brownian motion as κ approaches zero. The parameter setting in the numerical experiments is listed in Table 1.

For the implementation of all numerical experiments in this paper, we use a PC with AMD Ryzen 7 5800H CPU 16GB RAM and MATLAB R2021a as numerical computation software.

4.1 Computation of Mixed Moments

We compute mixed moments between the terminal value and the maximum of the NIG process by Propositions 2 and 3. Recall that they are obtained by the inverse Laplace transform of (3.4) in Proposition 2. To compute the inverse Laplace transform, we apply the Gaver-Stehfest algorithm. See Appendix A for the algorithm. Constants ω_- and ω_+ in (3.7) and (3.8) of Proposition 3 are set to -2 and 2, respectively. For the numerical integration of (3.7) and (3.8), we use the MATLAB function *quadgk*, which is the Gauss-Kronrod quadrature.

For comparison with our analytical method, Monte Carlo estimates of the mixed moments are calculated. In the Monte Carlo simulation, we generate sample paths of the NIG process as the subordinated Brownian motion sample paths on a fixed time grid, which is set at equal intervals. For simulating the NIG process, see Cont and Tankov (2003) for example. To reduce the convergence error, 10 million paths are generated for each estimate. We would like to emphasize that the setting of the time discretization is important for accurate Monte Carlo estimation of the moments of maximum. The estimates are always underestimated due to the time discretization error. In order to examine the degree of the error, the number of time steps per year is set to four patterns: $2^3, 2^7, 2^{11}$, and 2^{15}.

Figure 1 illustrates the numerical results of the mixed moments for the case of $T = 1$. The solid and dashed lines in the figure depict the levels of the moments calculated by our analytical method for the parameter settings of Cases 1 and 2, respectively. The dotted and chain lines plot the Monte Carlo estimates of the moments for Cases 1 and 2, respectively, with error bars[2]. The accuracy of the Monte Carlo estimates improves with increasing time steps, approaching the levels of the analytical moments. As we all know, the Monte Carlo simulation is very time-consuming. Computed in 2^{15} time steps, that is more than 13 hours. However, using our method, we can obtain the values of the six moments in each case within a total of one second.

[2]Since the standard errors are very small, the error bars in the figure may be too short to be discernible.

Figure 1: Moments of maximum of NIG process

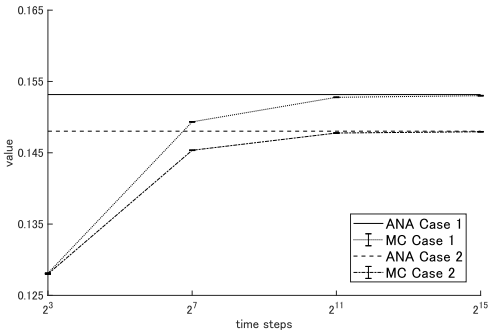

Panel A: 1st moment $m_{0,1}$

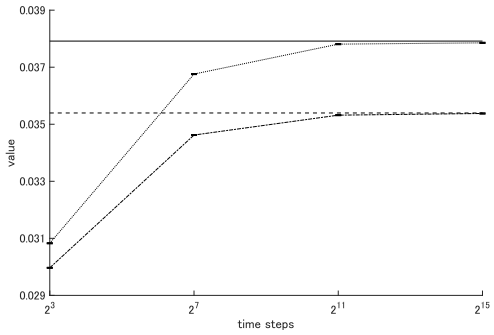

Panel B: 2nd moment $m_{0,2}$

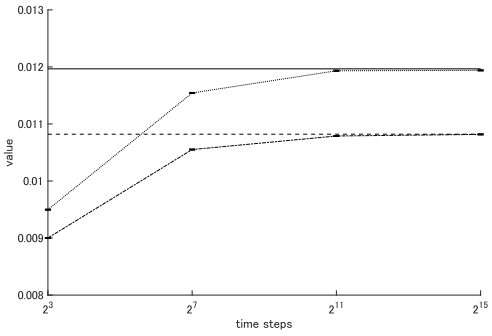

Panel C: 3rd moment $m_{0,3}$

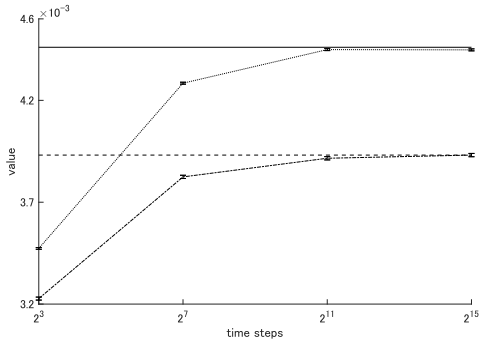

Panel D: 4th moment $m_{0,4}$

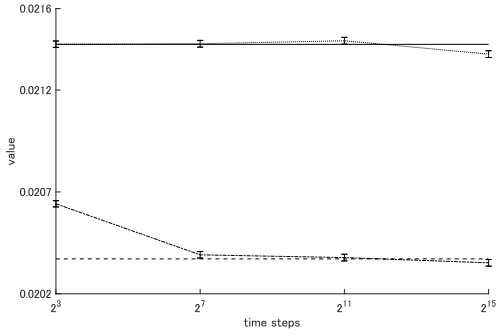

Panel E: (1,1)-th mixed moment $m_{1,1}$

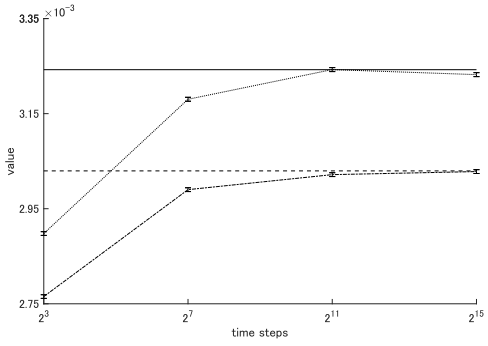

Panel F: (2,2)-th mixed moment $m_{2,2}$

4.2 Approximation of Density Function

In this subsection, we consider a two-dimensional cumulant expansion to the joint density function of the terminal value and the maximum of a Lévy process $(Y_T, \overline{Y}_T)$ around the joint density function of those of a Brownian motion $(Z_T, \overline{Z}_T)$.

Let g and $\hat{g}$ be the joint density functions of $(Y_T, \overline{Y}_T)$ and $(Z_T, \overline{Z}_T)$, respectively. Then g is approximated by

$$g(x,y) \sim \hat{g}(x,y) + \sum_{d=1}^{\infty} \sum_{n_1+n_2=d} \frac{I_{n_1,n_2}(\kappa)}{n_1! n_2!} (-1)^d \left(\partial_{n_1,n_2} \hat{g}\right)(x,y), \tag{4.3}$$

where $\kappa := (c_{l_1,l_2} - \hat{c}_{l_1,l_2})_{l_1,l_2 \geq 0}$, and the mapping I_{n_1,n_2} is defined in (B.3) of Appendix B.2. Here, c_{l_1,l_2} and $\hat{c}_{l_1,l_2}$ denote the (l_1,l_2)-th mixed cumulants of $(Y_T, \overline{Y}_T)$ and $(Z_T, \overline{Z}_T)$, respectively. Any mixed cumulant can be expressed as a polynomial of mixed moments, and vice versa. The relationship between the cumulants and the moments is shown in Appendix B.1 and B.2. The derivation of (4.3) can be found in Appendix B.3.

The joint density function of the terminal value and the maximum of a Brownian motion with parameters a, b is known in the form

$$\hat{g}(x,y) = \sqrt{\frac{2}{\pi}} \frac{e^{-\frac{a^2}{2b^2}T}}{\left(b^2 T\right)^{3/2}} (2y - x)\, e^{\frac{a}{b^2}x - \frac{(2y-x)^2}{2b^2 T}}, \quad x \leq y. \tag{4.4}$$

See Borodin and Salminen (2015) for the derivation of (4.4). The closed-form expression of the partial derivative $\left(\partial_{n_1,n_2} \hat{g}\right)(x,y)$ in (4.3) is provided in Appendix C.

Combining (4.3) with our moment calculation method, we expect to obtain an approximation for the joint density function of $(Y_T, \overline{Y}_T)$. In numerical experiments, the approximate marginal density functions with respect to the maximum $\overline{Y}_T$ of the NIG process are calculated. The NIG parameters are set to Cases 1 and 2 in Table 1 with $T = 1$. When applying (4.3), we choose the parameters a, b in (4.4) such that the first and second moments of the maximum of the Brownian motion are equal to those of the NIG process. That is,

$$\underset{a \in \mathbf{R}, b > 0}{\arg\min} \left(\hat{m}_{0,1} - m_{0,1}\right)^2 + \left(\hat{m}_{0,2} - m_{0,2}\right)^2.$$

We then calculate the third and fourth order approximations of the density function. To check the validity of the approximate density functions, we compare them with the density function estimated by a Monte Carlo simulation using 10 million sample paths with 2^{15} time steps per year.

Figure 2 shows a plot of the approximate density functions. The solid lines in the figure depict the density functions of the maximum of the Brownian motion moment-matched to the maximum of the NIG process. The dashed and chain lines denote the third and fourth order approximate density functions, respectively. However, these lines are indistinguishable, because they are almost equal to the density functions of the maximum of the Brownian motion. In other words, the third and fourth order terms in (4.3) have little effect on the shape of the approximate density functions. The bar charts represent the density functions estimated by the Monte Carlo simulation. As can be seen from the figure, the approximate density functions cannot capture the left side of the estimated density functions, that is, the part where the density changes discontinuously near zero. The convergence of the approximate density functions to the true density function is very slow.

In order to improve the accuracy, we need to consider an appropriate density function different from (4.4). Probably, a density function with an atom at zero is a candidate. For now, however, this is a subject for future research.

Figure 2: Approximate density functions of maximum of NIG process

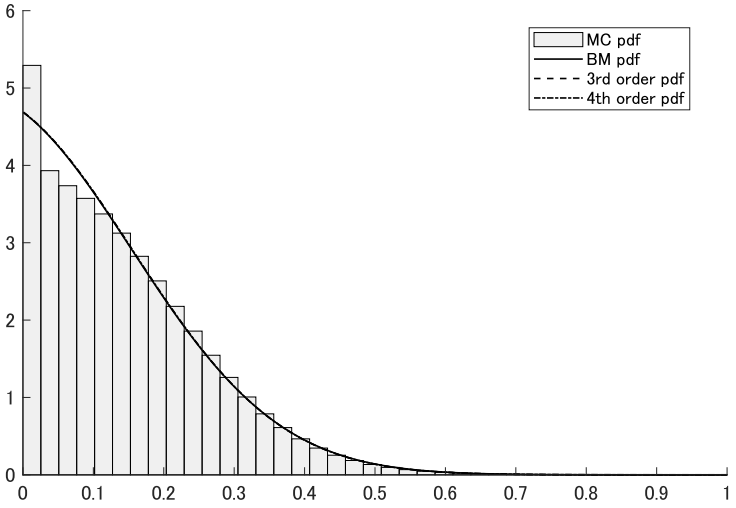

Panel A: Case 1

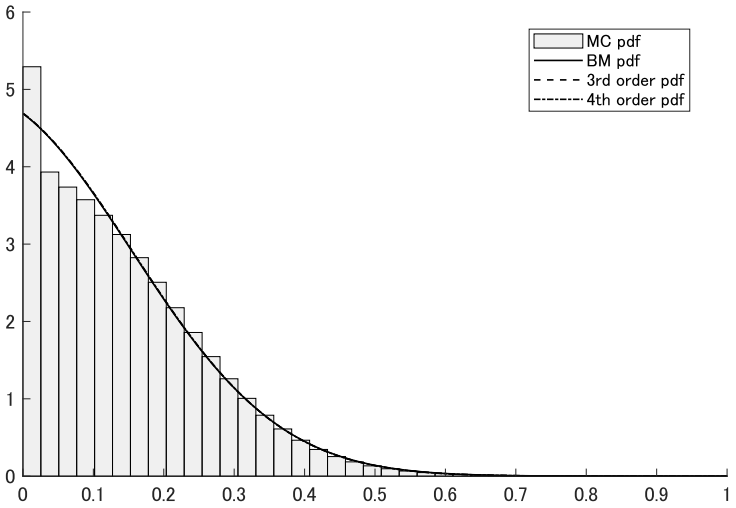

Panel B: Case 2

5 Application to Option Pricing

In the previous section, it is shown that our analytical method yields very accurate moments of the maximum of a Lévy process. However, the approximate density functions based on the moments are inaccurate. Although not discussed here, we have applied the approximate density function to option pricing, but the results, which we will provide upon request, were not good. In this section, we attempt another application of our moment calculation method to option pricing, *the Monte Carlo simulation with moment-matching samples.*

5.1 Moment-Matching Samples

Let

$$\left(\overline{Y}_{[1]}, \overline{Y}_{[2]}, \ldots, \overline{Y}_{[J]}\right), \tag{5.1}$$

be a random sample vector from the maximum of a Lévy process, $\overline{Y}_T$, where J denotes the number of sampling in a Monte Carlo simulation. We transform the random samples (5.1) to match the first and second moments of the underlying population by defining

$$\overline{Y}^*_{[j]} = \sqrt{\frac{m_{0,2} - m_{0,1}^2}{\Sigma}} \left(\overline{Y}_{[j]} - M\right) + m_{0,1}, \quad \text{for } j = 1, 2, \ldots, J, \tag{5.2}$$

where M and Σ are the sample mean and the sample variance of (5.1), respectively. Recall that the population moments $m_{0,1}$ and $m_{0,2}$ are obtained by our analytical method. In the following, we use the moment-matching samples

$$\left(\overline{Y}^*_{[1]}, \overline{Y}^*_{[2]}, \ldots, \overline{Y}^*_{[J]}\right),$$

to evaluate barrier and lookback options.

5.2 Option Pricing

In this subsection, we briefly explain the pricing of barrier and lookback options where the payoff depends on the maximum value of an underlying asset price process.

Assume frictionless markets and the absence of arbitrage opportunities. We consider the probability measure $\mathbb{Q}$ as a risk-neutral measure. Suppose that an underlying asset price process $(S_t)_{t\geq 0}$ under the risk-neutral measure is given by

$$S_t = S_0 e^{Y_t}, \quad \text{for every } t \geq 0, \tag{5.3}$$

where Y_t is defined by (4.1). Parameter r in (4.1) is interpreted as an instantaneous risk-free rate. Note that the discounted asset price process $(e^{-rt}S_t)_{t\geq 0}$ is an $\mathbb{F}$-martingale. The maximum of the underlying asset price in finite time interval $[0, T]$ is written as

$$\overline{S}_T := \sup_{0\leq t\leq T} S_t = S_0 e^{\overline{Y}_T}.$$

The price of an option that has a payoff function $H(S_T, \overline{S}_T)$ and expires at T can be represented as

$$\mathbb{E}\left[e^{-rT} H(S_T, \overline{S}_T)\right] = e^{-rT}\mathbb{E}\left[h(Y_T, \overline{Y}_T)\right], \tag{5.4}$$

where $h(y, \overline{y}) := H(S_0 e^y, S_0 e^{\overline{y}})$. Therefore, we only need to evaluate the expected payoff $\mathbb{E}\left[h(Y_T, \overline{Y}_T)\right]$ by the Monte Carlo simulation with moment-matching samples to obtain the option price. In numerical experiments, three types of options are addressed as follows.

Example 1 (Up-and-out put) An up-and-out put option is a type of barrier options. The payoff with maturity T, strike price K, and barrier level L is

$$H(S_T, \overline{S}_T) = (K - S_T)^+ \mathbf{1}_{\{\overline{S}_T < L\}}.$$

Equivalently,

$$h(Y_T, \overline{Y}_T) = S_0(e^k - e^{Y_T})\mathbf{1}_{\{Y_T < k\}}\mathbf{1}_{\{\overline{Y}_T < l\}},$$

where $k := \ln K/S_0$ and $l := \ln L/S_0$.

Example 2 (Fixed-strike lookback call) A fixed-strike lookback call option is a type of lookback options. The payoff with maturity T and fixed strike price K is

$$H(S_T, \overline{S}_T) = (\overline{S}_T - K)^+.$$

Equivalently,

$$h(Y_T, \overline{Y}_T) = S_0(e^{\overline{Y}_T} - e^k)\mathbf{1}_{\{\overline{Y}_T > k\}}.$$

Example 3 (Floating-strike lookback put) A floating-strike lookback put option is also a type of lookback options. The payoff with maturity T is

$$H(S_T, \overline{S}_T) = \overline{S}_T - S_T.$$

Equivalently,

$$h(Y_T, \overline{Y}_T) = S_0(e^{\overline{Y}_T} - e^{Y_T}).$$

5.3 Numerical Experiments

The purpose of this subsection is to see to what extent the Monte Carlo simulation with moment-matching samples can reduce the discretization errors in barrier and lookback option pricing. Adopting the NIG process (4.2) as the driving factor of the underlying asset price, we calculate the prices of up-and-out put, fixed-strike call, and floating-strike put options. The parameters of the model are Cases 1 and 2 in Table 1, the initial price of the underlying asset is $S_0 = 100$, and the maturity of all options is $T = 1$. The conditions for the Monte Carlo simulation are the same as in Section 4.1. That is, 10 million sample paths are generated for each option pricing, and the numbers of time steps per year are set to 2^3, 2^7, 2^{11}, and 2^{15}. For comparison, we also evaluate these option prices by the Monte Carlo simulation without moment-matching samples.

Tables 2 and 3 show the prices of up-and-out put options in Cases 1 and 2, respectively. These options have strike prices $K = 100$, 110, and 120 and barrier levels $L = 105$ and 110. In the tables, MCMM and MC denote the results of the Monte Carlo simulation with and without moment-matching samples, respectively. The values in parentheses are the standard errors of the estimated prices. Recall that the larger the number of time steps, the smaller the discretization error, but the longer the computation time. In our estimation, the discretization errors almost disappear in 2^{15} time steps. As can be seen from the tables, the discretization errors of MCMM are smaller than those of MC. Even with 2^7 time steps, the Monte Carlo simulation with moment-matching samples yields option prices that are acceptable accuracy for practical use. On the other hand, the Monte Carlo simulation without moment-matching samples requires at least 2^{11} time steps to obtain option prices

with the same level of accuracy as MCMM with 2^7 time steps. Therefore, by applying our simulation method, we can achieve a significant reduction in computation time. Incidentally, the computation time for 2^7 time steps is about 140 seconds, while that for 2^{11} time steps is more than 28 minutes.

Tables 4 and 5 show the prices of lookback options in Cases 1 and 2, respectively. In the tables, FIC represents fixed-strike call options, and FLP denotes floating-strike put options. The strike prices of the fixed-strike call options are $K = 100$, 110, and 120. It can be seen from the tables that our simulation method dramatically reduces the discretization errors in lookback option pricing. In most cases of MCMM, only 2^3 time steps are sufficient to obtain accurate option prices. The computation time for 2^3 time steps is only 40 seconds. In contrast to MCMM, the Monte Carlo simulation without moment-matching samples produces large discretization errors in such cases.

We conduct the same numerical experiments under the variance gamma (VG) process, which is also one of the most popular Lévy processes in finance applications. That is, the VG process is adopted as $(X_t)_{t\geq 0}$ in (4.1). The characteristic exponent of the VG process is

$$\psi_X(\theta) = \frac{1}{\kappa} \ln \left(1 + \frac{1}{2}\sigma^2 \kappa \theta^2 - i\mu\kappa\theta \right), \tag{5.5}$$

where σ, μ, κ are some constants. This process is a time-changed Brownian motion subordinated by the gamma process. It has a finite variation with infinite small jumps, but relatively low activity. The parameters of the VG process play a similar role to those of the NIG process. The values of the VG parameters are taken from Table 1.

Figures 3 and 4 plot the prices of up-and-out put and lookback options, respectively, with error bars. From the figures, it can be seen that our simulation method can sufficiently reduce the discretization errors, even when the VG process is employed.

6 Conclusion

This paper proposes an analytical method to calculate mixed moments between the terminal value and the maximum of a Lévy process. This method is applicable to the class of Lévy processes with the Boyarchenko-Levendorskiĭ representation. Numerical experiments show that our analytical method provides sufficiently accurate values of the mixed moments. However, we also find that the convergence of the approximate density function based on the moments is very slow.

As an application of our moment calculation method, we propose a Monte Carlo simulation with moment-matching samples to evaluate barrier and lookback options with continuous monitoring. The numerical results show that our simulation method can reduce the time discretization error. In particular, the error in the estimates of the lookback option prices is dramatically reduced. Hence, by using our simulation method in financial practice, the computation time for option pricing can be greatly reduced.

Our moment calculation method should be a general-purpose tool for a variety of applications. Future research directions will include applications to fields other than option pricing, such as physics, economics, and insurance.

A Gaver-Stehfest Algorithm

This appendix briefly explains the Gaver-Stehfest algorithm proposed by Stehfest (1970), which is for the computation of the inverse Laplace transform. This algorithm is straight-

Table 2: Up-and-out put option prices under NIG process (Case 1)

			time steps			
K	L		2^3	2^7	2^{11}	2^{15}
100	105	MCMM	0.781	0.718	0.714	0.716
			(0.001)	(0.001)	(0.001)	(0.001)
		MC	0.883	0.743	0.717	0.716
			(0.001)	(0.001)	(0.001)	(0.001)
110	105	MCMM	2.061	1.881	1.871	1.874
			(0.002)	(0.002)	(0.002)	(0.002)
		MC	2.398	1.959	1.880	1.877
			(0.002)	(0.002)	(0.002)	(0.002)
120	105	MCMM	4.109	3.723	3.704	3.708
			(0.003)	(0.003)	(0.003)	(0.003)
		MC	4.931	3.899	3.724	3.714
			(0.003)	(0.003)	(0.003)	(0.003)
100	110	MCMM	0.945	0.931	0.930	0.930
			(0.001)	(0.001)	(0.001)	(0.001)
		MC	0.991	0.941	0.931	0.931
			(0.001)	(0.001)	(0.001)	(0.001)
110	110	MCMM	2.615	2.567	2.563	2.564
			(0.002)	(0.002)	(0.002)	(0.002)
		MC	2.786	2.602	2.567	2.565
			(0.002)	(0.002)	(0.002)	(0.002)
120	110	MCMM	5.499	5.373	5.365	5.366
			(0.003)	(0.003)	(0.003)	(0.003)
		MC	5.977	5.467	5.376	5.370
			(0.003)	(0.003)	(0.003)	(0.003)

Table 3: Up-and-out put option prices under NIG process (Case 2)

			time steps			
K	L		2^3	2^7	2^{11}	2^{15}
100	105	MCMM	0.941	0.883	0.879	0.879
			(0.001)	(0.001)	(0.001)	(0.001)
		MC	1.071	0.907	0.882	0.880
			(0.001)	(0.001)	(0.001)	(0.001)
110	105	MCMM	2.169	2.031	2.024	2.023
			(0.002)	(0.002)	(0.002)	(0.002)
		MC	2.511	2.091	2.030	2.025
			(0.002)	(0.002)	(0.002)	(0.002)
120	105	MCMM	4.131	3.855	3.845	3.842
			(0.003)	(0.003)	(0.003)	(0.003)
		MC	4.886	3.982	3.857	3.846
			(0.003)	(0.003)	(0.003)	(0.003)
100	110	MCMM	1.190	1.169	1.166	1.166
			(0.001)	(0.001)	(0.001)	(0.001)
		MC	1.249	1.179	1.167	1.167
			(0.001)	(0.001)	(0.001)	(0.001)
110	110	MCMM	2.833	2.777	2.773	2.774
			(0.002)	(0.002)	(0.002)	(0.002)
		MC	3.001	2.806	2.776	2.775
			(0.002)	(0.002)	(0.002)	(0.002)
120	110	MCMM	5.631	5.504	5.496	5.498
			(0.003)	(0.003)	(0.003)	(0.003)
		MC	6.037	5.571	5.503	5.500
			(0.003)	(0.003)	(0.003)	(0.003)

Table 4: Lookback option prices under NIG process (Case 1)

			time steps			
Type	K		2^3	2^7	2^{11}	2^{15}
FIC	100	MCMM	17.435	17.432	17.432	17.432
			(0.005)	(0.005)	(0.005)	(0.005)
		MC	14.526	16.984	17.387	17.413
			(0.005)	(0.005)	(0.005)	(0.005)
FIC	110	MCMM	9.559	9.581	9.581	9.581
			(0.004)	(0.004)	(0.004)	(0.004)
		MC	7.789	9.291	9.553	9.566
			(0.004)	(0.004)	(0.004)	(0.004)
FIC	120	MCMM	4.913	4.875	4.872	4.873
			(0.003)	(0.003)	(0.003)	(0.003)
		MC	3.853	4.700	4.857	4.862
			(0.003)	(0.003)	(0.003)	(0.003)
FLP		MCMM	14.384	14.379	14.381	14.407
			(0.003)	(0.004)	(0.004)	(0.004)
		MC	11.476	13.930	14.336	14.388
			(0.004)	(0.004)	(0.004)	(0.004)

Table 5: Lookback option prices under NIG process (Case 2)

			time steps			
Type	K		2^3	2^7	2^{11}	2^{15}
FIC	100	MCMM	16.772	16.771	16.771	16.771
			(0.005)	(0.005)	(0.005)	(0.005)
		MC	14.463	16.459	16.741	16.762
			(0.005)	(0.005)	(0.005)	(0.005)
FIC	110	MCMM	8.968	8.978	8.980	8.978
			(0.004)	(0.004)	(0.004)	(0.004)
		MC	7.591	8.781	8.960	8.973
			(0.004)	(0.004)	(0.004)	(0.004)
FIC	120	MCMM	4.431	4.399	4.398	4.398
			(0.003)	(0.003)	(0.003)	(0.003)
		MC	3.640	4.285	4.387	4.395
			(0.003)	(0.003)	(0.003)	(0.003)
FLP		MCMM	13.723	13.725	13.723	13.739
			(0.004)	(0.004)	(0.004)	(0.004)
		MC	11.414	13.414	13.693	13.730
			(0.004)	(0.004)	(0.004)	(0.004)

Figure 3: Up-and-out put option prices under VG process

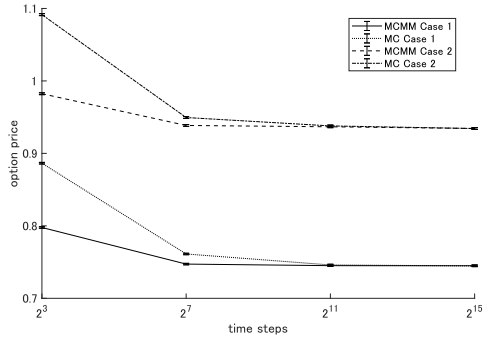

Panel A: $K = 100$, $L = 105$

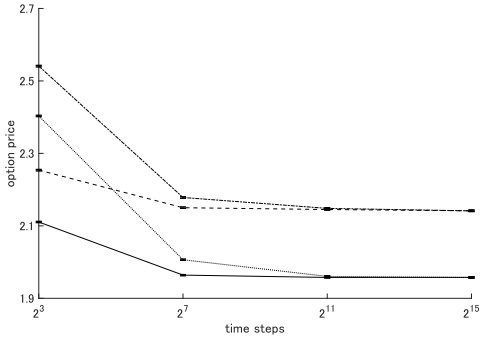

Panel B: $K = 110$, $L = 105$

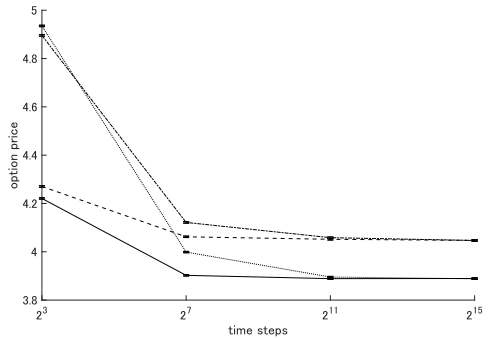

Panel C: $K = 120$, $L = 105$

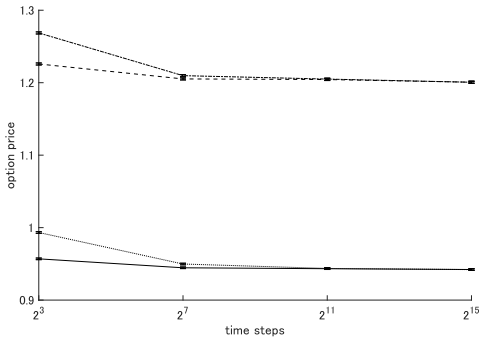

Panel D: $K = 100$, $L = 110$

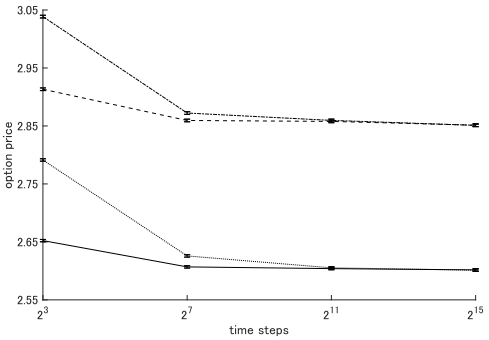

Panel E: $K = 110$, $L = 110$

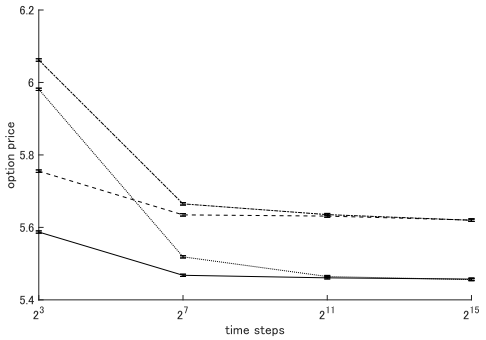

Panel F: $K = 120$, $L = 110$

Figure 4: Lookback option prices under VG process

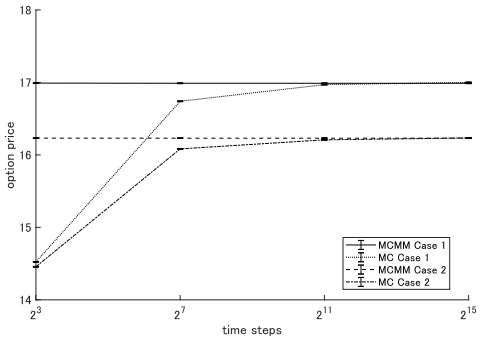

Panel A: FIC with $K = 100$

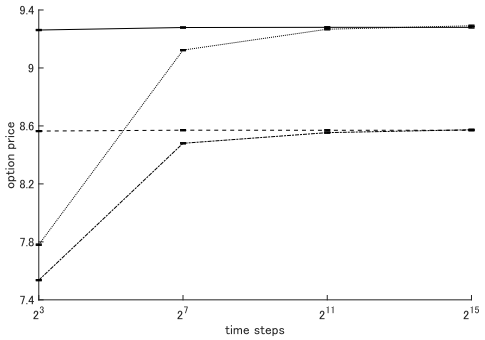

Panel B: FIC with $K = 110$

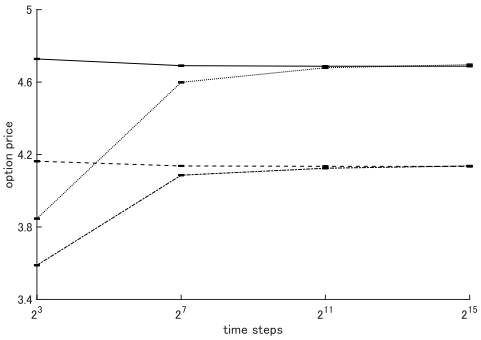

Panel C: FIC with $K = 120$

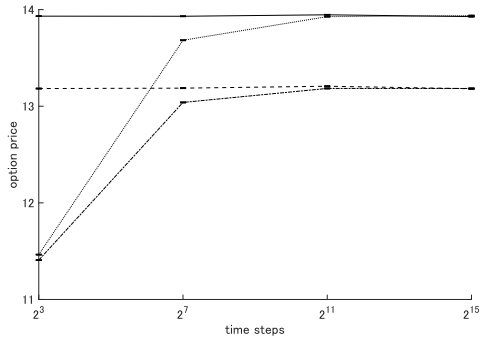

Panel D: FLP

forward. For any bounded real-valued function f defined on $[0,\infty)$ that is continuous at y, the inverse Laplace transform $\tilde{f}$ of f is given by

$$\tilde{f}(x) = \lim_{p\to\infty} \frac{1}{2\pi i} \int_{c-ip}^{c+ip} e^{xy} f(y) dy = \lim_{n\to\infty} \tilde{f}_n(x),$$

where $c > 0$ is a constant, and

$$\tilde{f}_n(x) := \frac{\ln 2}{x} \frac{(2n)!}{n!(n-1)!} \sum_{k=0}^{n} (-1)^k \frac{n!}{k!(n-k)!} f\left((n+k)\frac{\ln 2}{x}\right).$$

To accelerate the convergence, an n-point Richardson extrapolation is applicable. More precisely, $\tilde{f}$ can be approximated by f_n^* for sufficiently large n, where

$$f_n^*(x) := \sum_{k=1}^{n} (-1)^{n-k} \frac{k^n}{k!(n-k)!} \tilde{f}_k(x).$$

See Stehfest (1970) for details.

B Cumulant Expansion to Joint Density Function

This appendix provides a general formula for the cumulant expansion to an arbitrary two-dimensional joint density function around a known density function.

Suppose that there are arbitrary mixed moments and cumulants of a pair of random variables (X, Y), all of which are finite. Let $\phi_{X,Y}$ be the joint characteristic function of (X, Y). Then the mixed moments $(m_{n_1,n_2})_{n_1,n_2\geq 0}$ of (X, Y) are defined as constants satisfying the following equation:

$$\phi_{X,Y}(\theta_1, \theta_2) = 1 + \sum_{d=1}^{\infty} \sum_{n_1+n_2=d} \frac{m_{n_1,n_2}}{n_1! n_2!} (i\theta_1)^{n_1} (i\theta_2\ )^{n_2}, \quad \text{for } \theta_1, \theta_2 \in \mathbf{R}. \tag{B.1}$$

On the other hand, the mixed cumulants $(c_{n_1,n_2})_{n_1,n_2\geq 0}$ of (X, Y) are defined as constants satisfying the following equation:

$$\ln \phi_{X,Y}(\theta_1, \theta_2) = \sum_{d=1}^{\infty} \sum_{n_1+n_2=d} \frac{c_{n_1,n_2}}{n_1! n_2!} (i\theta_1)^{n_1} (i\theta_2\ )^{n_2}, \quad \text{for } \theta_1, \theta_2 \in \mathbf{R}. \tag{B.2}$$

B.1 Cumulants as Polynomials of Moments

Applying the Taylor expansion to $\ln \phi_{X,Y}(\theta_1, \theta_2)$ combined with (B.1) and comparing it with (B.2), we obtain the following relations:

- $n_1 + n_2 = 0$ or 1

$$c_{0,0} = 0, \quad c_{1,0} = m_{1,0}, \quad c_{0,1} = m_{0,1}.$$

- $n_1 + n_2 = 2$

$$c_{2,0} = -m_{1,0}^2 + m_{2,0}, \quad c_{1,1} = -m_{1,0} m_{0,1} + m_{1,1}, \quad c_{0,2} = -m_{0,1}^2 + m_{0,2}.$$

- $n_1 + n_2 = 3$

$$\begin{aligned}
c_{3,0} &= 2m_{1,0}^3 - 3m_{1,0}m_{2,0} + m_{3,0},\\
c_{2,1} &= 2m_{0,1}m_{1,0}^2 - 2m_{1,0}m_{1,1} - m_{0,1}m_{2,0} + m_{2,1},\\
c_{1,2} &= 2m_{0,1}^2 m_{1,0} - m_{0,2}m_{1,0} - 2m_{0,1}m_{1,1} + m_{1,2},\\
c_{0,3} &= 2m_{0,1}^3 - 3m_{0,1}m_{0,2} + m_{0,3}.
\end{aligned}$$

- $n_1 + n_2 = 4$

$$\begin{aligned}
c_{4,0} &= -6m_{1,0}^4 + 12m_{1,0}^2 m_{2,0} - 3m_{2,0}^2 - 4m_{1,0}m_{3,0} + m_{4,0},\\
c_{3,1} &= -6m_{0,1}m_{1,0}^3 + 6m_{1,0}^2 m_{1,1} + 6m_{0,1}m_{1,0}m_{2,0} - 3m_{1,1}m_{2,0} - 3m_{1,0}m_{2,1} - m_{0,1}m_{3,0} + m_{3,1},\\
c_{2,2} &= -6m_{0,1}^2 m_{1,0}^2 + 2m_{0,2}m_{1,0}^2 + 8m_{0,1}m_{1,0}m_{1,1} - 2m_{1,1}^2 - 2m_{1,0}m_{1,2}\\
&\quad + 2m_{0,1}^2 m_{2,0} - m_{0,2}m_{2,0} - 2m_{0,1}m_{2,1} + c_{2,2},\\
c_{1,3} &= -6m_{0,1}^3 m_{1,0} + 6m_{0,1}m_{0,2}m_{1,0} - m_{0,3}m_{1,0} + 6m_{0,1}^2 m_{1,1} - 3m_{0,2}m_{1,1} - 3m_{0,1}m_{1,2} + m_{1,3},\\
c_{0,4} &= -6m_{0,1}^4 + 12m_{0,1}^2 m_{0,2} - 3m_{0,2}^2 - 4m_{0,1}m_{0,3} + m_{0,4}.
\end{aligned}$$

B.2 Moments as Polynomials of Cumulants

Applying the Taylor expansion to $\exp\left(\ln \phi_{X,Y}(\theta_1, \theta_2)\right)$ combined with (B.2) and comparing it with (B.1), we obtain the following relations:

- $n_1 + n_2 = 0$ or 1

$$m_{0,0} = 1, \quad m_{1,0} = c_{1,0}, \quad m_{0,1} = c_{0,1}.$$

- $n_1 + n_2 = 2$

$$m_{2,0} = c_{1,0}^2 + c_{2,0}, \quad m_{1,1} = c_{1,0}c_{0,1} + c_{1,1}, \quad m_{0,2} = c_{0,1}^2 + c_{0,2}.$$

- $n_1 + n_2 = 3$

$$\begin{aligned}
m_{3,0} &= c_{1,0}^3 + 3c_{1,0}c_{2,0} + c_{3,0}, \quad m_{2,1} = c_{0,1}c_{1,0}^2 + 2c_{1,0}c_{1,1} + c_{0,1}c_{2,0} + c_{2,1},\\
m_{1,2} &= c_{0,1}^2 c_{1,0} + c_{0,2}c_{1,0} + 2c_{0,1}c_{1,1} + c_{1,2}, \quad m_{0,3} = c_{0,1}^3 + 3c_{0,1}c_{0,2} + c_{0,3}.
\end{aligned}$$

- $n_1 + n_2 = 4$

$$\begin{aligned}
m_{4,0} &= c_{1,0}^4 + 6c_{1,0}^2 c_{2,0} + 3c_{2,0}^2 + 4c_{1,0}c_{3,0} + c_{4,0},\\
m_{3,1} &= c_{0,1}c_{1,0}^3 + 3c_{1,0}^2 c_{1,1} + 3c_{0,1}c_{1,0}c_{2,0} + 3c_{1,1}c_{2,0} + 3c_{1,0}c_{2,1} + c_{0,1}c_{3,0} + c_{3,1},\\
m_{2,2} &= c_{0,1}^2 c_{1,0}^2 + c_{0,2}c_{1,0}^2 + 4c_{0,1}c_{1,0}c_{1,1} + 2c_{1,1}^2 + 2c_{1,0}c_{1,2}\\
&\quad + c_{0,1}^2 c_{2,0} + c_{0,2}c_{2,0} + 2c_{0,1}c_{2,1} + c_{2,2},\\
m_{1,3} &= c_{0,1}^3 c_{1,0} + 3c_{0,1}c_{0,2}c_{1,0} + c_{0,3}c_{1,0} + 3c_{0,1}^2 c_{1,1} + 3c_{0,2}c_{1,1} + 3c_{0,1}c_{1,2} + c_{1,3},\\
m_{0,4} &= c_{0,1}^4 + 6c_{0,1}^2 c_{0,2} + 3c_{0,2}^2 + 4c_{0,1}c_{0,3} + c_{0,4}.
\end{aligned}$$

We represent the above relations by the following mapping.

$$I_{n_1,n_2} : c = (c_{l_1,l_2})_{l_1,l_2 \geq 0} \longmapsto I_{n_1,n_2}(c) = m_{n_1,n_2}. \tag{B.3}$$

B.3 Approximate Density Function

Suppose that a pair of random variables (X, Y) has a joint density function g, but its closed-form representation is unknown. Let $\hat{g}$ be a known joint density function of a pair of random variables (Z, W). Since

$$\ln \frac{\phi_{X,Y}(\theta_1, \theta_2)}{\phi_{Z,W}(\theta_1, \theta_2)} = \sum_{d=1}^{\infty} \sum_{n_1+n_2=d} \frac{c_{n_1,n_2} - \hat{c}_{n_1,n_2}}{n_1! n_2!} (i\theta_1)^{n_1} (i\theta_2)^{n_2},$$

we have

$$\begin{aligned}
\phi_{X,Y}(\theta_1, \theta_2) &= \exp\left\{ \sum_{d=1}^{\infty} \sum_{n_1+n_2=d} \frac{c_{n_1,n_2} - \hat{c}_{n_1,n_2}}{n_1! n_2!} (i\theta_1)^{n_1} (i\theta_2)^{n_2} \right\} \phi_{Z,W}(\theta_1, \theta_2) \\
&= \left\{ 1 + \sum_{d=1}^{\infty} \sum_{n_1+n_2=d} \frac{I_{n_1,n_2}(\kappa)}{n_1! n_2!} (i\theta_1)^{n_1} (i\theta_2)^{n_2} \right\} \phi_{Z,W}(\theta_1, \theta_2) \\
&= \phi_{Z,W}(\theta_1, \theta_2) + \sum_{d=1}^{\infty} \sum_{n_1+n_2=d} \frac{I_{n_1,n_2}(\kappa)}{n_1! n_2!} (i\theta_1)^{n_1} (i\theta_2)^{n_2} \phi_{Z,W}(\theta_1, \theta_2), \quad \text{(B.4)}
\end{aligned}$$

where $\kappa := (c_{l_1,l_2} - \hat{c}_{l_1,l_2})_{l_1,l_2 \geq 0}$, and I_{n_1,n_2} is defined in (B.3). Applying the inverse Fourier transform to the both sides of (B.4), we have

$$\begin{aligned}
g(x, y) &= \frac{1}{(2\pi)^2} \int_{-\infty}^{+\infty} \int_{-\infty}^{+\infty} e^{-ix\theta_1 - iy\theta_2} \phi_{X,Y}(\theta_1, \theta_2) d\theta_1 d\theta_2 \\
&= \frac{1}{(2\pi)^2} \int_{-\infty}^{+\infty} \int_{-\infty}^{+\infty} e^{-ix\theta_1 - iy\theta_2} \phi_{Z,W}(\theta_1, \theta_2) d\theta_1 d\theta_2 \\
&\quad + \sum_{d=1}^{\infty} \sum_{n_1+n_2=d} \frac{I_{n_1,n_2}(\kappa)}{n_1! n_2!} \frac{1}{(2\pi)^2} \int_{-\infty}^{+\infty} \int_{-\infty}^{+\infty} e^{-ix\theta_1 - iy\theta_2} (i\theta_1)^{n_1} (i\theta_2)^{n_2} \phi_{Z,W}(\theta_1, \theta_2) d\theta_1 d\theta_2 \\
&= \hat{g}(x, y) + \sum_{d=1}^{\infty} \sum_{n_1+n_2=d} \frac{I_{n_1,n_2}(\kappa)}{n_1! n_2!} (-1)^d \left(\partial_{n_1,n_2} \hat{g}\right)(x, y).
\end{aligned}$$

C Partial Derivative of (4.4)

The joint density function (4.4) can be rewritten as

$$\hat{g}(x, y) = A e^{\frac{a}{b^2} x} z e^{-z^2}, \quad \text{for } x \leq y.$$

Here, we put

$$A := \frac{2}{\sqrt{\pi} b^2 T} e^{-\frac{a^2}{2b^2} T},$$

and define the function $z := z(x, y) = (2y - x)/\lambda$, where $\lambda := \sqrt{2b^2 T}$. Then it holds

$$\begin{aligned}
\left(\partial_{n_1,n_2} \hat{g}\right)(x, y) &= A \frac{\partial^{n_1}}{\partial x^{n_1}} \left[e^{\frac{a}{b^2} x} \frac{\partial^{n_2}}{\partial y^{n_2}} z e^{-z^2} \right] \\
&= A \frac{\partial^{n_1}}{\partial x^{n_1}} \left[e^{\frac{a}{b^2} x} \frac{(-1)^{n_2}}{2} H_{n_2+1}(z) e^{-z^2} \left(\frac{2}{\lambda}\right)^{n_2} \right] \\
&= \frac{A}{2} \left(\frac{-2}{\lambda}\right)^{n_2} \sum_{m=0}^{n_1} \binom{n_1}{m} \left(\frac{a}{b^2}\right)^m e^{\frac{a}{b^2} x} \left(\frac{1}{\lambda}\right)^{n_1-m} H_{n_1+n_2-m+1}(z) e^{-z^2},
\end{aligned}$$

where $H_n(x)$ denotes the n-th Hermite polynomial.

References

[1] Avramidis, A. and L'Ecuyer, P. Efficient Monte Carlo and quasi-Monte Carlo option pricing under the variance gamma model. *Management Science*, 52(12):1930–1944, 2006.

[2] Avramidis, A., L'Ecuyer, P., and Tremblay, P. A. Efficient simulation of gamma and variance-gamma processes. In *Winter Simulation Conference*, pages 319–326, 2003.

[3] Barndorff-Nielsen, O. Processes of normal inverse Gaussian type. *Finance and Stochastics*, 2(1):41–68, 1997.

[4] Becker, M. Unbiased Monte Carlo valuation of lookback, swing and barrier options with continuous monitoring under variance gamma models. *Journal of Computational Finance*, 13(4):35–61, 2010.

[5] Borodin, A. and Salminen, P. *Handbook of Brownian Motion - Facts and Formulae, Second Edition*. Birkhäuser, 2015.

[6] Boyarchenko, S. and Levendorskiĭ S. *Non-Gaussian Merton-Black-Scholes Theory*. World Scientific, 2002.

[7] Carr, P. and Wu, L. The finite moment log stable process and option pricing. *Journal of Finance*, 58(2):753–777, 2003.

[8] Carr, P., Geman, H., Madan, D., and Yor, M. The fine structure of asset returns: An empirical investigation. *Journal of Business*, 75(2):305–332, 2002.

[9] Cont, R. and Tankov, P. *Financial Modelling with Jump Processes*. Chapman and Hall/CRC, 2003.

[10] Eraker, B. Do stock prices and volatility jump? Reconciling evidence from spot and option prices. *Journal of Finance*, 59(3):1367–1403, 2004.

[11] Eraker, B., Johannes, M., and Polson, N. The impact of jumps in volatility and returns. *Journal of Finance*, 58(3):1269–1300, 2003.

[12] Feng, L. and Linetsky, V. Pricing discretely monitored barrier options and defaultable bonds in Lévy process models: a fast Hilbert transform approach. *Mathematical Finance*, 18(3):337–384, 2008.

[13] Fusai, G. and Meucci, A. Pricing discretely monitored Asian options under Lévy processes. *Journal of Banking & Finance*, 32(10):2076–2088, 2008.

[14] Jönsson, H. and Schoutens, W. Single name credit default swaptions meet single sided jump models. *Review of Derivatives Research*, 11(1):153–169, 2008.

[15] Kou, S. A jump-diffusion model for option pricing. *Management Science*, 48(8):1086–1101, 2002.

[16] Madan, D. and Schoutens, W. Break on through to the single side. *Available at SSRN 1003144*, 2007.

[17] Madan, D. and Seneta, E. The variance gamma (VG) model for share market returns. *Journal of Business*, pages 511–524, 1990.

[18] Madan, D., Carr, P., and Chang, E. The variance gamma process and option pricing. *Review of Finance*, 2(1):79–105, 1998.

[19] Merton, R. Option pricing when underlying stock returns are discontinuous. *Journal of Financial Economics*, 3(1-2):125–144, 1976.

[20] Ozeki, T., Umezawa, Y., Yamazaki, A., and Yoshikawa, D. An extension of Credit-Grades model approach with Lévy processes. *Quantitative Finance*, 11(12):1825–1836, 2011.

[21] Ribeiro, C. and Webber, N. Valuing path-dependent options in the variance-gamma model by Monte Carlo with a gamma bridge. *Journal of Computational Finance*, 7(2):81–100, 2004.

[22] Sato, K. *Lévy Processes and Infinitely Divisible Distributions*. Cambridge University Press, 1999.

[23] Schoutens, W. The meixner process: Theory and applications in finance. *Working Paper*, 2002.

[24] Shiraya, K., Uenishi, H., and Yamazaki, A. A general control variate method for Lévy models in finance. *European Journal of Operational Research*, 284(3):1190–1200, 2020.

[25] Shiraya, K., Wang, C., and Yamazaki, A. A general control variate method for time-changed Lévy processes: An application to option pricing. *Available at Center for Advanced Research in Finance, Faculty of Economics, University of Tokyo*, 2021.

[26] Stehfest, H. Algorithm 368: Numerical inversion of Laplace transforms. *Communications of the ACM*, 13(1):47–49, 1970.

[27] Umezawa, Y. and Yamazaki, A. Pricing path-dependent options with discrete monitoring under time-changed Lévy processes. *Applied Mathematical Finance*, 22(2):133–161, 2015.

[28] Yamazaki, A. Pricing average options under time-changed Lévy processes. *Review of Derivatives Research*, 17(1):79–111, 2014.